PARAMETRIC ANALYSES OF AN ABSORPTION REFRIGERATION SYSTEM WITH WATER AND LITHIUM BROMIDE IN STEADY STATE POWERED BY SOLAR ENERGY

V. Prendin[a],
L. C. Martinez[b]
and N. M. S. Kaminari[c]

[a]Pontifícia Universidade Católica do Paraná
Departamento de Engenharia Mecânica
Bairro Prado Velho
CEP. 80215-901, Curitiba, Paraná, Brasil
prendinvitor@gmail.com
[b]Pontifícia Universidade Católica do Paraná
Departamento de Engenharia Mecânica
Bairro Prado Velho
CEP. 80215-901, Curitiba, Paraná, Brasil
leonardo.cavalheiro@pucpr.br
[c]Pontifícia Universidade Católica do Paraná
Departamento de Engenharia Mecânica
Bairro Prado Velho
CEP. 80215-901, Curitiba, Paraná, Brasil
nice.kaminari@pucpr.br

Received: Mar 07, 2022
Revised: Mar 25, 2022
Accepted: Mar 26, 2022

ABSTRACT

The demand of energy utilization is increasing expressively as fast as the development of countries. Besides being available everywhere and virtual inexhaustible, renewable energy is undoubtedly necessary to avoid depleting the planet's natural resources and global warming. Even considering the primordially environmental importance, the result of no emissions by renewable energy grant attractive also for political and economics statement. It should be noted the sun is the most abundant primary energy source in the planet and essential for eco-friendly process like photosynthesis, wind action, water cycle as well direct uses as electric and thermal generations. Consequently, nowadays several methodologies have been applied in order to transfer energy between the cycle and its surroundings optimizing for instance the coefficient of performance and heat exchangers. An absorption system is widely applied in these cases due to supply a unique solution for a range of technological problems from solar cooling to steam-driven refrigeration. Alternatively, this article main objective is modulating an absorption refrigeration system (ARS) which uses water-lithium bromide as a working fluid. Therefore, using the software Engineering Equation Solver (EES) is possible to obtain a thermodynamic single effect code that allows elaborating parametric analyses. In other words, performed and verified the influence of some input parameters over other output parameters. First, it was necessary to consider the cycle operating as reversible and steady state. Furthermore, it is assumed that no chemical reactions occur between water and lithium bromide. Thus, in the meantime apply the heat exchangers and a Solar Collector to receive the thermal energy and provide to the refrigeration cycle. Similarly, water from external sources was used to change heat with the fluid water-lithium bromide. Satisfactory results were founded and it enable to calculate and evaluate all system heat transfers rates and coefficient of performance. Almost all of input parameters introduced brought adequate values over output parameters, but the most convenient were: mass balance of water-lithium bromide solution and temperature of cold water from outside source. Clearly, results always can be found but in conclusion this article can be used to verify parameters sensitivity, optimized absorption refrigeration solutions and supply knowledge for future applications.

Keywords: renewable energy, absorption refrigeration systems, engineering equation solver, refrigeration cycle, water-lithium bromide

NOMENCLATURE

A_{cs}	solar collectors' area, m²
C_p	water specific heat, J/kg°C
COP	coefficient of performance, %
E_{cs}	useful energy, kWh
h_1	enthalpy flow of refrigerant fluid in the exit of the Absorber and in the entrance of the Pump, kg/s
h_2	enthalpy flow of refrigerant fluid in the exit of the Pump and in the entrance of the Heat Exchanger, kg/s
h_3	enthalpy flow of refrigerant fluid in the exit of the Heat Exchanger and in the entrance of the Thermal Generator, kg/s
h_4	enthalpy flow of refrigerant fluid in the exit of the Thermal Generator and in the entrance of the Heat Exchanger, kg/s
h_5	enthalpy flow of refrigerant fluid in the exit of the Thermal Generator and in the entrance of the Expansion Valve, kg/s
h_6	enthalpy flow of refrigerant fluid in the exit of the Expansion Valve and in the entrance of the Absorber, kg/s
h_7	enthalpy flow of refrigerant fluid in the exit of the Thermal Generator and in the entrance of the Condenser, kg/s
h_8	enthalpy flow of refrigerant fluid in the exit of the Condenser and in the entrance of the Expansion Valve, kg/s

h_9 enthalpy flow of refrigerant fluid in the exit of the Expansion Valve and in the entrance of the Evaporator, kg/s

h_{10} enthalpy flow of refrigerant fluid in the exit of the Evaporator and in the entrance of the Absorber, kg/s

h_{11} enthalpy flow in the entrance of hot water from the Solar Collector, kg/s

h_{12} enthalpy flow in the exit of hot water from the Solar Collector, kg/s

h_{13} enthalpy flow in the entrance of condensation water from the external source, kg/s

h_{14} enthalpy flow in the entrance of condensation water from the external source, kg/s

h_{15} enthalpy flow of refrigerant fluid in the entrance of condensation water from the external source, kg/s

h_{16} enthalpy flow of refrigerant fluid in the exit of condensation water from the external source, kg/s

h_{17} enthalpy flow of refrigerant fluid in the entrance of cold water from the external source, kg/s

h_{18} enthalpy flow of refrigerant fluid in the exit of cold water from the external source, kg/s

I average of solar normal irradiations in Brasilia, kWh/m²day

K Solar Collector efficiency, %

$\dot{m}_1$ mass flow of refrigerant fluid in the exit of the Absorber and in the entrance of the Pump, kg/s

$\dot{m}_2$ mass flow of refrigerant fluid in the exit of the Pump and in the entrance of the Heat Exchanger, kg/s

$\dot{m}_3$ mass flow of refrigerant fluid in the exit of the Heat Exchanger and in the entrance of the Thermal Generator, kg/s

$\dot{m}_4$ mass flow of refrigerant fluid in the exit of the Thermal Generator and in the entrance of the Heat Exchanger, kg/s

$\dot{m}_5$ mass flow of refrigerant fluid in the exit of the Thermal Generator and in the entrance of the Expansion Valve, kg/s

$\dot{m}_6$ mass flow of refrigerant fluid in the exit of the Expansion Valve and in the entrance of the Absorber, kg/s

$\dot{m}_7$ mass flow of refrigerant fluid in the exit of the Thermal Generator and in the entrance of the Condenser, kg/s

$\dot{m}_8$ mass flow of refrigerant fluid in the exit of the Condenser and in the entrance of the Expansion Valve, kg/s

$\dot{m}_9$ mass flow of refrigerant fluid in the exit of the Expansion Valve and in the entrance of the Evaporator, kg/s

$\dot{m}_{10}$ mass flow of refrigerant fluid in the exit of the Evaporator and in the entrance of the Absorber, kg/s

$\dot{m}_{11}$ mass flow in the entrance of hot water from the Solar Collector, kg/s

$\dot{m}_{12}$ mass flow in the exit of hot water from the Solar Collector, kg/s

$\dot{m}_{13}$ mass flow in the entrance of condensation water from the external source, kg/s

$\dot{m}_{14}$ mass flow in the entrance of condensation water from the external source, kg/s

$\dot{m}_{15}$ mass flow of refrigerant fluid in the entrance of condensation water from the external source, kg/s

$\dot{m}_{16}$ mass flow of refrigerant fluid in the exit of condensation water from the external source, kg/s

$\dot{m}_{17}$ mass flow of refrigerant fluid in the entrance of cold water from the external source, kg/s

$\dot{m}_{18}$ mass flow of refrigerant fluid in the exit of cold water from the external source, kg/s

$\dot{Q}_a$ heat transfer rate rejected by the Absorber, kW

$\dot{Q}_c$ heat transfer rate rejected by the Condenser, kW

$\dot{Q}_e$ heat transfer rate absorbed by the Evaporator, kW

$\dot{Q}_g$ heat transfer rate absorbed by the Thermal Generator, kW

$\dot{Q}_{tc}$ heat transfer rate that occurs between the hot and the cold side of the Heat Exchanger, kW

T_1 temperature of refrigerant fluid in the exit of the Absorber and in the entrance of the Pump, °C

T_2 temperature of refrigerant fluid in the exit of the Pump and in the entrance of the Heat Exchanger, °C

T_3 temperature of refrigerant fluid in the exit of the Heat Exchanger and in the entrance of the Thermal Generator, °C

T_4 temperature of refrigerant fluid in the exit of the Thermal Generator and in the entrance of the Heat Exchanger, °C

T_5 temperature of refrigerant fluid in the exit of the Thermal Generator and in the entrance of the Expansion Valve, °C

T_6 temperature of refrigerant fluid in the exit of the Expansion Valve and in the entrance of the Absorber, °C

T_7 temperature of refrigerant fluid in the exit of the Thermal Generator and in the entrance of the Condenser, °C

T_8 temperature of refrigerant fluid in the exit of the Condenser and in the entrance of the Expansion Valve, °C

T_9 temperature of refrigerant fluid in the exit of the Expansion Valve and in the entrance of the Evaporator, °C

T_{10} temperature of refrigerant fluid in the exit of the Evaporator and in the entrance of the Absorber, °C

$$\sum_e \dot{m}_e = \sum_s \dot{m}_s \tag{1.1}$$

$$\frac{dE_{vc}}{dt} = \dot{Q}_{vc} - \dot{W}_{vc} + \sum_e \dot{m}_e \left(h_e + \frac{V_e^2}{2} + g.z_e \right) - \sum_s \dot{m}_s \left(h_s + \frac{V_s^2}{2} + g.z_s \right) \tag{2}$$

$$\dot{Q}_{vc} = -\dot{W}_{vc} + \sum_s \dot{m}_s \left(h_s + \frac{V_s^2}{2} + g.z_s \right) - \sum_e \dot{m}_e \left(h_e + \frac{V_e^2}{2} + g.z_e \right) \tag{2.1}$$

$$\dot{Q}_{vc} = -\dot{W}_{vc} + \sum_s \dot{m}_s (h_s) - \sum_e \dot{m}_e (h_e) \tag{2.2}$$

where $\frac{dm_{vc}}{dt}$, $\sum_e \dot{m}_e$, $\sum_s \dot{m}_s$ are the temporal rate of mass variation in the control volume and the sum of input and output mass flow, respectively. Additionally, $\frac{dE_{vc}}{dt}$, $\dot{W}_{vc}$, h, $\frac{V^2}{2}$ and z are the temporal rate of energy variation in the control volume, pump work, enthalpy flow, kinetic energy and gravitational potential, respectively. The kinetic and potential energy variations are neglected. Finally, $\dot{Q}_{vc}$, $\dot{W}_{vc}$ are the net heat transfer energy rate in the control volume and the net energy transfer rate per work in the control volume, respectively.

Below, the main equations for all components that guide the absorption refrigeration system are described separately.

Evaporator

In the Evaporator, a heat exchange occurs between the refrigerant fluid and the cold water that is coming from the external source, Equations (3) e (4). Thus, heat is absorbed by the ARS and the mixture of liquid and water vapor are converted into saturated water vapor. Therefore, the energy balance in the Evaporator is given by Equation (5).

$$\dot{m}_9 = \dot{m}_{10} \tag{3}$$

$$\dot{m}_{17} = \dot{m}_{18} \tag{4}$$

$$\dot{Q}_e = \dot{m}_{10} h_{10} - \dot{m}_9 h_9 \tag{5}$$

where $\dot{m}_9, \dot{m}_{10}, h_{10}, h_9$ are the mass and enthalpy flow of refrigerant fluid in the entrance and exit of the Evaporator. On the other hands, $\dot{m}_{17}, \dot{m}_{18}$ are the mass flow in the entrance and exit of cold water from the external source.

The heat transfer rate $\dot{Q}_e$ occurs simultaneously between the Evaporator and the external source, Equation (6). Consequently, the logarithmic mean temperature difference (LMTD) method is used according to Equation (7) to modulate this component.

$$\dot{Q}_e = UA_e \Delta T_{lm,e} \tag{6}$$

$$\Delta T_{lm,e} = \frac{(T_{17} - T_{10}) - (T_{18} - T_9)}{\ln \frac{(T_{15} - T_8)}{(T_{16} - T_8)}} \tag{7}$$

Condenser

In the Condenser, a heat exchange occurs between the refrigerant fluid and the condensation water that is coming from the external source, Equations (8) e (9). Thus, heat is released by the ARS and the superheated water vapor is converted into saturated liquid water. Therefore, the energy balance in the Condenser is given by Equation (10).

$$\dot{m}_7 = \dot{m}_8 \tag{8}$$

$$\dot{m}_{15} = \dot{m}_{16} \tag{9}$$

$$\dot{Q}_c = \dot{m}_8 h_8 - \dot{m}_7 h_7 \tag{10}$$

where $\dot{m}_7, \dot{m}_8, h_7, h_8$ are the mass and enthalpy flow of refrigerant fluid in the entrance and exit of the Condenser. On the other hands, $\dot{m}_{15}, \dot{m}_{16}$ are the mass flow in the entrance and exit of condensation water from the external source.

The heat transfer rate, $\dot{Q}_c$, occurs simultaneously between the Condenser and the external source, Equation (11). Consequently, the logarithmic mean temperature difference (LMTD) method is used according to Equation (12) to modulate this component.

$$\dot{Q}_c = UA_c \Delta T_{lm,c} \tag{11}$$

$$\Delta T_{lm,c} = \frac{(T_{15} - T_8) - (T_{16} - T_8)}{\ln \frac{(T_{15} - T_8)}{(T_{16} - T_8)}} \tag{12}$$

Absorber

In the Absorber, a heat exchange occurs between the refrigerant fluid and the condensation water that is coming from the external source, Equation (13) and Equation (15). Thus, heat is released by the ARS and the weak solution of water vapor is absorbed by a strong solution of water-lithium bromide which flows back to the Absorber. The Equation (14) represents the product of mass flow versus strong, x_1 and weak, x_6,

concentration of lithium bromide solution. The energy balance in the Absorber is given by Equation (16).

$$\dot{m}_1 = \dot{m}_6 + \dot{m}_{10} \quad (13)$$

$$\dot{m}_1 x_1 = \dot{m}_6 x_6 \quad (14)$$

$$\dot{m}_{13} = \dot{m}_{14} \quad (15)$$

$$\dot{Q}_a = \dot{m}_{10} h_{10} + \dot{m}_6 h_6 - \dot{m}_1 h_1 \quad (16)$$

where $\dot{m}_6, \dot{m}_{10}, h_6, h_{10}$ are the mass and enthalpy flow of refrigerant fluid in the entrance of the Absorber. While $\dot{m}_1, h_1$ are the mass and enthalpy flow of refrigerant fluid in the exit of the Absorber, $\dot{m}_{13}, \dot{m}_{14}$ are the mass flow in the entrance and exit of condensation water from the external source.

The heat transfer rate, $\dot{Q}_a$, given by Equation (17), occurs simultaneously between the Absorber and the external source. Consequently, the logarithmic mean temperature difference (LMTD) method is used according to Equation (18) to modulate this component.

$$\dot{Q}_a = UA_a \Delta T_{lm,a} \quad (17)$$

$$\Delta T_{lm,a} = \frac{(T_6 - T_{14}) - (T_1 - T_{13})}{\ln \frac{(T_6 - T_{14})}{(T_1 - T_{13})}} \quad (18)$$

Thermal Generator

In the Thermal Generator, a heat exchange occurs between the refrigerant fluid and the hot water that is coming from the Solar Collector, Equation (19) and Equation (20). Thus, heat is absorbed by the ARS and it occurs the vaporization of water present in the lithium bromide solution. Assuming the vapor that leaves the Thermal Generator is free of salt, the Equation (21) represents the product of mass flow versus concentration, x_3 and x_4, of lithium bromide solution. Therefore, the energy balance in the Thermal Generator is given by Equation (22).

$$\dot{m}_3 = \dot{m}_4 + \dot{m}_7 \quad (19)$$

$$\dot{m}_{11} = \dot{m}_{12} \quad (20)$$

$$\dot{m}_3 x_3 = \dot{m}_4 x_4 \quad (21)$$

$$\dot{Q}_g = \dot{m}_4 h_4 + \dot{m}_7 h_7 - \dot{m}_3 h_3 \quad (22)$$

where $\dot{m}_4, \dot{m}_7, \dot{m}_3, h_4, h_7, h_3$ are the mass and enthalpy flow of refrigerant fluid in the entrance and exit of the Thermal Generator. On other hands, $\dot{m}_{11}, \dot{m}_{12}$ are the mass flow in the entrance and exit of hot water from the Solar Collector.

The heat transfer rate, $\dot{Q}_g$, given by Equation (23), occurs simultaneously between the Thermal Generator and the Solar Collector. Consequently, the logarithmic mean temperature difference (LMTD) method is used according to Equation (24) to modulate this component.

$$\dot{Q}_g = UA_g \Delta T_{lm,g} \quad (23)$$

$$\Delta T_{lm,g} = \frac{(T_{11} - T_4) - (T_{12} - T_7)}{\ln \frac{(T_{11} - T_4)}{(T_{12} - T_7)}} \quad (24)$$

Heat Exchanger

In the Heat Exchanger, a heat exchange occurs between the strong LiBr solution that is returning from the Thermal Generator and the subcooled liquid solution that is flowing to the Thermal Generator. Thus, heat is absorbed by the ARS and the mixture of liquid and water vapor are converted into saturated water vapor. Therefore, the energy balance in the Heat Exchanger is between a cold, $\dot{Q}_{tcf}$ and hot, $\dot{Q}_{tcq}$, side that is given by Equation (25) and Equation (26).

$$\dot{Q}_{tcq} = \dot{m}_4 h_4 + \dot{m}_5 h_5 \quad (25)$$

$$\dot{Q}_{tcf} = \dot{m}_3 h_3 - \dot{m}_2 h_2 \quad (26)$$

where $\dot{m}_4, \dot{m}_5, h_4, h_5$ are the mass and enthalpy flow of refrigerant fluid in exit of the Thermal Generator and $\dot{m}_3, \dot{m}_2, h_3, h_2$ are the mass and enthalpy flow of refrigerant fluid in the entrance of the Thermal Generator. Admittedly in this case, mass flow is constant for each side of Heat Exchanger. Thus, the effectiveness of this Heat Exchanger is given by Equation (27).

$$\varepsilon_{tc} = \frac{T_4 - T_5}{T_4 - T_2} \quad (27)$$

Herold (2016) affirms the logarithmic mean temperature difference (LMTD) method is used according to Equation (29) to modulate this component.

$$\dot{Q}_{tc} = UA_{tc} \Delta T_{lm,tc} \quad (28)$$

$$\Delta T_{lm,tc} = \frac{(T_4 - T_3) - (T_5 - T_2)}{\ln \frac{(T_4 - T_3)}{(T_5 - T_2)}} \quad (29)$$

Pump and Expansion Valve

In this ARS, while pump increases the pressure level, expansion valve decreases. Thus, both components are considered as ideal and the process as isentropic. Therefore, the temperature remains constant and the energy balance in the Pump is given by Equation (30).

$$\dot{W}_b = \dot{m}_2 h_2 - \dot{m}_1 h_1 \quad (30)$$

Solar Collector

Moreira (2019) affirms that is possible to quantify a useful thermal energy of input, E_{cs}, in the system absorbed by the Solar Collector through the Equation (31).

$$E_{cs} = \frac{V * C_p * (T_4 - T_{19})}{3600} \quad (31)$$

where V, C_p are the water volume to be heated and the specific heat of water, respectively. On the other hands, T_4, T_{19} are the temperature of the hot water required by the Thermal Generator and the average temperature of Brasilia (Cresesb, 2017).

Alternatively, the area of Solar Collectors, A_{cs}, can be obtained through Equation (32) proposed by Ghodeshwar (2018).

$$A_{cs} = \frac{\dot{Q}_g}{KI} \quad (32)$$

where $\dot{Q}_g$, K, I are the heat transfer rate in the Thermal Generator, the efficiency of the Solar Collector and the average of solar normal irradiations in Brasilia, respectively.

Coefficient of Performance

The coefficient of performance, COP, is determined by the ratio between the desired effect over the energy supply and can be obtained through the Equation (33).

$$COP = \frac{\dot{Q}_e}{\dot{Q}_{gv}} \quad (33)$$

RESULTS AND DISCUSSION

A set of operating conditions for a single-effect water/lithium bromide cycle with Heat Exchangers in Table 1 was based on (Herold, 2016) and generated by imposing mass and energy balances on the components as listed in mathematical equations.

The hardware schematic in Table 2 provides additional details on some of the key assumptions used in modeling this cycle. The pump work is negligible in this case because it is quite small as compared with the heat transfer rates associated with the other components. The total of fourteen input parameters was varied to obtain successful results found by (Herold, 2016). Besides, the author varied each input parameter nine times to obtain the thermodynamic behaviors. It should be noted that each input parameter has different increment according to their own units.

Table 1. Set of Operating Conditions (Herold, 2016).

State Points	h (kJ/kg)	$\dot{m}$ (kg/s)	P (kPa)	Vapor Quality	T (°C)	x (% LiBr)
1	85.8	0.05	0.68	0	32.9	56.7
2	85.8	0.05	7.353		32.9	56.7
3	147	0.05	7.353		63.2	56.7
4	221.2	0.0455	7.353	0	89.4	62.4
5	153.9	0.0455	7.353		53.2	62.4
6	153.9	0.0455	0.68	0.006	44.7	62.4
7	2643.3	0.0455	7.353		76.8	0
8	167.2	0.0455	7.353	0	39.9	0
9	167.2	0.0455	0.68	0.064	1.5	0
10	2503.2	0.0455	0.68	1	1.5	0
11	419.1	1			100	
12	404.4				96.5	
13	104.8	0.28			25	
14	154.9				37	
15	104.8	0.28			25	
16	144.8				34.6	
17	42	0.4			10	
18	15.6				3.7	

Table 2. Hardware Schematic.

Baseline Inputs Defining Single-Effect Operating Conditions in Table 1		Variation of Input Parameters for Parametric Analyses			Baseline Outputs Defining Single-Effect Operating Conditions in Table 1	
Input Parameter	Value	First Value	Increment	Final Value	Output Parameter	Value
ε_{tc}	0.64	0.56	0.02	0.72	$\Delta T_{lm,c}$ (K)	9.34
$\dot{m}_1$ (kg/s)	0.05	0.03	0.005	0.07	$\Delta T_{lm,g}$ (K)	14.674
UA_a (kW/K)	1.8	1.4	0.1	2.2	$\Delta T_{lm,a}$ (K)	7.8
UA_c (kW/K)	1.2	0.8	0.1	1.6	$\Delta T_{lm,e}$ (K)	4.7
UA_g (kW/K)	1	0.6	0.1	1.4	$\Delta T_{lm,tc}$ (K)	23.15
UA_e (kW/K)	2.25	1.85	0.1	2.65	$\dot{Q}_a$ (kW)	14.04
T_{13} (°C)	25	21	1	29	$\dot{Q}_e$ (kW)	10.575
$\dot{m}_{13}$ (kg/s)	0.28	0.26	0.005	0.3	$\dot{Q}_{tc}$ (kW)	3.062
T_{15} (°C)	25	21	1	29	$\dot{Q}_c$ (kW)	11.209
$\dot{m}_{15}$ (kg/s)	0.28	0.26	0.005	0.3	$\dot{Q}_g$ (kW)	14.67
T_{11} (°C)	100	96	1	104	COP	0.721
$\dot{m}_{11}$ (kg/s)	1	0.98	0.005	1.02	$\dot{W}_b$ (kW)	0.206
T_{17} (°C)	10	6	1	14		
$\dot{m}_{17}$ (kg/s)	0.4	0.38	0.005	0.42		

After adding increments of 0.005 °C for nine times, it was possible to verify the influence of $\dot{m}_1$. Then, the increases of $\dot{Q}_g, \dot{Q}_a$ and decreases of COP are noted in Figure 3. It happens because the heat flow that is absorbed by the Thermal Generator increases, while the heat flow absorbed by the Evaporator does not have significant changes.

After adding increments of 0,1 kW/K for nine times, it was possible to verify the same influence of all thermal conductance's UA_a, UA_c, UA_g and UA_e. It happens because by increasing the material's ability to conduct heat, the logarithmic mean temperature difference between the fluids from external sources and the H_2O-LiBr fluid is raised.

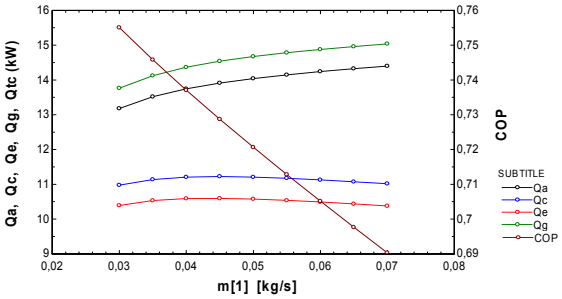

Figure 3. Behavior of entrance mass flow parameter.

Then, the increases of $\dot{Q}_e, \dot{Q}_g, \dot{Q}_a, \dot{Q}_c$ and the low reduction of COP are noted in Figure 4 represented by UA_g parameter.

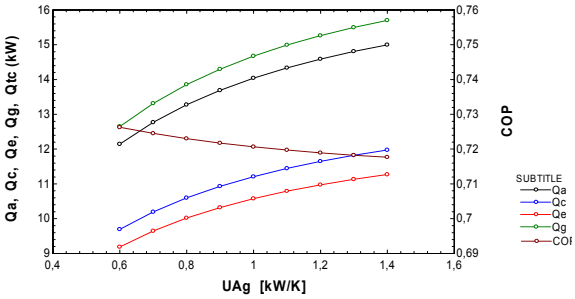

Figure 4. Behavior of Thermal Generator UA parameter.

After adding increments of 1ºCfor nine times, it was possible to verify the influence of T_{17}. Then, the increases of $\dot{Q}_e, \dot{Q}_g, \dot{Q}_a, \dot{Q}_c$ and COP are noted in Figure 5. It happens because the evaporation temperature and the heat flow absorbed in the Evaporator are increased when the temperature of cold water is raised. As a result, it will have more saturated water vapor being absorbed by the LiBr solution and more heat being absorbed in the Thermal Generator.

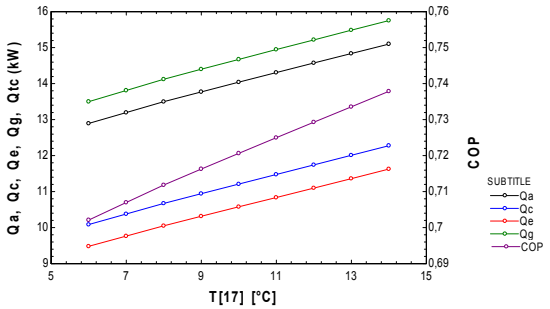

Figure 5. Behavior of cold water temperature parameter.

Heat exchangers with indirect contact as used in the system do not mix fluids from external sources with the H_2O-LiBr fluid. Therefore, there were not significant increases in the mass flow of refrigerant vapor caused by external sources $\dot{m}_{13}, \dot{m}_{15}, \dot{m}_{11}, \dot{m}_{17}$. However, it was undoubtedly necessary to verify the influence of T_{11} after adding increments of 1□ for nine times. Then, the increases of $\dot{Q}_e, \dot{Q}_g, \dot{Q}_a, \dot{Q}_c$ and the low variation of COP are noted in Figure 6. It happens because when the temperature of Thermal Generator hot water is raised, it will have as a result a solution more concentrated returning to the Absorber and more quantity of steam flowing to the Condenser.

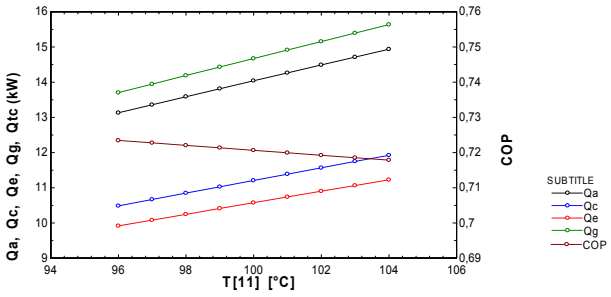

Figure 6. Behavior of Thermal Generator hot water temperature parameter.

After adding increments of 1ºCfor nine times, it was possible to verify the same influence of condensation water temperature T_{13} and T_{15} over the decreasing of $\dot{Q}_e, \dot{Q}_g, \dot{Q}_a, \dot{Q}_c$ and COP. It happens because the lower condensation water temperature T_{13}, the greater the water vapor absorption capacity from the Evaporator. On the other hands, as the condensation water leaves the Absorber at a higher temperature, the heat transfer capacity in the Condenser is reduced. The behavior of these results can be visualized graphically by Fig. 7 and 8.

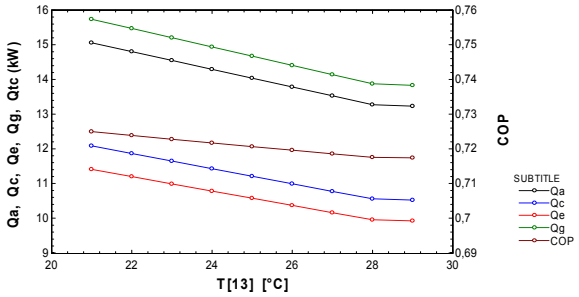

Figure 7. Behavior of Absorber condensation water temperature parameter.

The parametric analysis of hot water temperature T_4 required by the Thermal Generator is an adaptation to the cycle proposed by Herold (2016. Therefore, it is the last parameter to be analyzed and varied between 80 to 94 ºC in increments of 2ºC. There was an increase in the useful energy, E_{cs}, absorbed by the Solar Collector and also an increase in the area, A_{cs}, of Solar Collectors required as shown in Fig. 9.

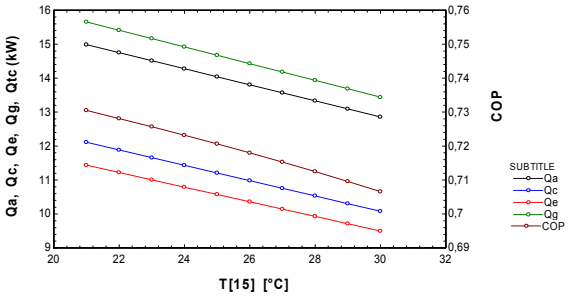

Figure 8. Behavior of Condenser condensation water temperature parameter.

It happens because the higher the water temperature required by the Thermal Generator, the greater the number of Solar Collectors to absorb the necessary thermal energy that will be used to supply the refrigeration cycle.

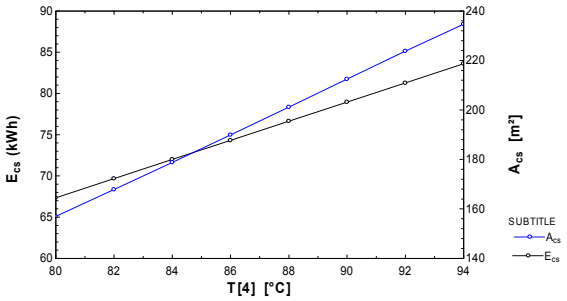

Figure 9. Behavior of hot water temperature required by the Thermal Generator.

CONCLUSIONS

After all results considered, there are no doubts about notable variations of input parameters over output parameters. However, the most relevant were: mass flow of the H_2O-LiBr solution and the temperature of cold water, T_{17}. Besides, it was possible to conclude that the temperatures from external sources should be considered one of the most sensitive parameters to the absorption refrigeration system especially because it was showed different behaviors in the heat transfer rate and in the COP.

The data's introduced in the Solar Collector area and the useful energy can be used in future works to determine the quantity of Solar Collectors necessary to supply the system, the economic viability and the time lag between investment and payback. Another suggestion would be to analyze the viscosity as an input parameter since it also depends on the system temperature but was not included in this work.

Although, the general objectives were successfully attended and clearly the parametric analyses allowed to verify, validate and perform the single-effect absorption refrigeration system proposed by Herold (2016). In conclusion, the sensitivity of the values found demonstrate the crucial importance of accomplish a parametric analysis to optimize thermal engineering projects.

REFERENCES

Costa, E. C. Refrigeração. São Paulo. 3ª Edição. Editora Edgard Blucher Ltda, 1985.

CRESESB, SunData. Centro de Referência para Energia Solar e Eólica Sérgio Brito / CEPEL Potencial Solar. http://www.cresesb.cepel.br/index.php#data; 2017 (acessado 10 de Outubro 2020).

Ghodeshwar, A. Thermodynamic Analysis of Lithium Bromide-Water (LiBr-H2O) Vapor Absorption Refrigeration System Based on Solar Energy. v.5, p.1365-1371, 2018.

Herold, K. E. Absorption Chillers and Heat Pump, 2ª Edição, Editora CRC Press, 2016.

Moreira, S. Energias Renováveis, Geração Distribuída e Eficiência Energética. 1ª Edição. Editora LTC, 2019.

Pereira, E. B. Atlas Brasileiro de Energia Solar. INPE, 2ª Edição. São José dos Campos, 2017.

Reis, L. B. Energia, recursos naturais e a prática do desenvolvimento sustentável. 3ª Edição. Editora Manole Ltda, 2019.

Sonda INPE - Sistema de Organização Nacional de Dados Ambientais; http://sonda.ccst.inpe.br/; 2020 (acessado 13 de Outubro 2020).